

REVIEW PAPER

The Origin of Blue-Green Window and the Propagation of Radiation in Ocean Waters

A.T. Reghunath*, V. Venkataramanan, D. Victor Suvisheshamuthu, R. Krishnamohan, B. Raghavendra Prasad, S. Raghuv eer, C.K. Subramanian, P. Chandrasekhar and P.S. Narayanan

Department of Physics, Indian Institute of Science, Bangalore-560 012

and

M. Ravisankar, V.P.N. Nampoori and K. Sathianandan

Department of Physics, Cochin University of Science and Technology, Cochin-682 022

ABSTRACT

A review of the present knowledge about the origin of blue-green window in the attenuation spectrum of ocean waters is presented. The various physical mechanisms which contribute to the formation of the window are dealt separately and discussed. The typical values of attenuation coefficient arising out of the various processes are compiled to obtain the total beam attenuation coefficient. These values are then compared with measured values of attenuation coefficient for ocean waters collected from Arabian sea and Bay of Bengal. The region of minimum attenuation in pure particle-free sea water is found to be at 450 to 500 nm. It is shown that in the presence of suspended particles and chlorophyll, the window shifts to longer wavelength side. Some suggestions for future work in this area are also given in the concluding section.

1. INTRODUCTION

With the advent of lasers, there has been a revival of interest in the studies related to underwater applications. The acoustic waves and very low frequency electromagnetic waves are the commonly used sources in most underwater systems.

Received 24 April 1989, re-revised 11 April 1990.

* Present Address : Defence Science Centre, Delhi-110 054

Lasers have several advantages over other conventional sources because of their low divergence and high power. They therefore turn out to be ideal sources for underwater applications such as communication, target finding, ranging, etc. Advanced techniques have made it possible to obtain lasers of any desired wavelength.

As light propagates through the ocean water, it gets absorbed as well as scattered. The magnitude of the absorption and the scattering depends on the wavelength of light and the constituents of ocean water. The transmission of optical radiation in ocean water is found to be maximum at around 480 nm which is usually referred to as the blue-green window. The aim of this paper is to review the present knowledge about the absorption and scattering of light in ocean waters, including some of our work on Indian coastal waters. In addition, an attempt is made to explain some of the physics underlying the existence of the blue-green window in the medium.

A great deal of experimental and theoretical work on the transmission characteristics of optical radiation in pure and ocean waters¹⁻²³ has been reported in the past years. Several review articles have also been published on the optical properties of water. Notable among them are those by Irvine and Pollack²⁴ and by Hale and Querry²⁵. The various aspects of optical oceanography are compiled and published by different authors²⁶⁻²⁸. The effect of refractive index variation on the beam quality of a finite cross-section laser beam propagating in a sea water medium with temperature and salinity fluctuations is theoretically studied by Yura²⁹. The penetration of solar radiation in ocean waters and related optical properties of the ocean are also studied exhaustively by different workers^{30,31}. In this review those topics are not discussed as the scope of this paper is confined to attenuation of laser beams in ocean waters.

The attenuation of optical radiation in ocean water is a cumulative effect of a variety of phenomena such as absorption by water molecules and bio-organic constituents of ocean water, scattering by the density fluctuations in the medium and the suspended particulate matter in the water, etc. These topics are discussed in detail, in the following sections.

2. ABSORPTION OF LIGHT BY PURE WATER

The H_2O molecule has three fundamental modes of vibration, viz. ν_1 -symmetric, ν_2 -bending and ν_3 -antisymmetric. The corresponding frequencies in wave numbers are³²

$$\nu_1 : 3280 \text{ cm}^{-1} - 3.05 \mu\text{m}$$

$$\nu_2 : 1645 \text{ cm}^{-1} - 6.08 \mu\text{m}$$

$$\nu_3 : 3490 \text{ cm}^{-1} - 2.87 \mu\text{m}$$

Liquid water has very strong absorption at these frequencies. Robertson and Williams³³ have measured the absorption coefficient at the centre of the 3 μm band as 11900 cm^{-1} and at the 6 μm band as 2378 cm^{-1} . It is to be noted that the band at 3 μm is not a single band but a superposition of ν_1 , ν_3 and $2\nu_2$. In the region from 2 to 0.7 μm there exist several absorption bands for water, which are due to the harmonics and combinations of the fundamental. At higher harmonics the absorption bands of symmetric and antisymmetric vibrations overlap with each other. Tam and

Table 1 The absorption peaks for H_2O in the region 2 to 0.5 μm and their respective assignments (ν_v represents the stretching mode and ν_B the bending mode)

Peak of absorption band λ (μm)	Wave number ν (cm^{-1})	Absorption coefficient a (cm^{-1})	Assignment	Calculated* value of ν (cm^{-1})
1.94	5154	114	$\nu_v + \nu_B$	5202
1.45	6897	26	$2 \nu_v$	6988
1.19	8403	1.05	$2 \nu_v + \nu_B$	8498
0.97	10309	0.45	$3 \nu_v$	10293
0.85	11764	–	$3 \nu_v + \nu_B$	11803
0.76	13158	0.026	$4 \nu_v$	13472
0.604	16550	0.0023	$5 \nu_v$	16525
0.514	19460	0.00035	$6 \nu_v$	19452

* As per Tam and Patel¹⁴ [Eqn.(1)].

Patel¹⁴ observed the fifth and sixth harmonic of the $O-H$ stretch in the visible region of the spectrum and suggested the following anharmonic formula for the harmonic series of the $O-H$ stretch in water :

$$\nu^{(n)} = n (3620 - 63n) \text{ cm}^{-1} \quad (1)$$

The absorption bands observed by Curcio and Petty⁴ can be assigned to higher harmonics and combinations of the fundamental as shown in Table 1. The table shows the wavelength of peak absorption, corresponding wave number, magnitude of absorption coefficient, the assignment and the calculated value of wave number as per Eqn. (1).

The magnitude of the absorption coefficients given are those corresponding to the peaks in the absorption spectrum. The vibration in a real molecule will not be exactly simple harmonic but slightly anharmonic. The selection rules for an anharmonic oscillator are $\Delta v = \pm 1, \pm 2, \pm 3, \dots$, with diminishing probability. Therefore the absorption coefficients corresponding to higher harmonics will be smaller.

The real and imaginary parts of the refractive index of water, $n(\lambda)$ $k(\lambda)$ respectively, for the region 2 to 33 μm are reported by Rusk *et al.*³⁴ based on their reflectance measurements. The $k(\lambda)$, which is otherwise called the extinction coefficient, is related to the Lambert absorption coefficient $a(\lambda)$ by the relation,

$$a(\lambda) = \frac{4\pi k(\lambda)}{\lambda} \quad (2)$$

In 1972, Hale and Querry²⁵ tabulated the values of $n(\lambda)$ and $k(\lambda)$ of water for the region 200 nm to 200 μm , from a critical review of all the published data till that date.

It is more difficult to measure the absorption coefficient of water in the visible region than in the infrared, due to the very weak absorption in the visible region. A careful examination of the data on absorption coefficients available in the literature, reveals the existence of wide divergence in the values reported by various workers

(Table 2). Though there is a general agreement in the red side, in the 450 to 480 nm region there exists in certain cases, a disagreement by an order of magnitude. Most of these values, although claimed to be absorption coefficients, are actually attenuation coefficients (which is the sum of the intrinsic absorption and scattering coefficients), while in certain reports, the scattering losses have been calculated theoretically and subtracted. The disparities in these results are due to the very low value of absorption coefficient and therefore the experimental errors severely affect the measurements. Some of the possible experimental errors are :

- (a) In the pre-laser studies, insufficient collimation of light through cells of long path length;
- (b) Corrections for the reflections at the cell windows;
- (c) Temporal fluctuations in the intensity of the source; and
- (d) Difficulty in preparing high purity samples.

Table 2. Absorption coefficients of liquid H_2O near $25^\circ C$ at selected optical wavelengths, as given by various authors

Author	Absorption coefficient a (10^{-4} cm^{-1})						
	400 nm	450 nm	500 nm	550 nm	600 nm	650 nm	700 nm
James and Birge ¹	1.4	0.7	0.9	4	19	28	45
Clark and James ²	4.1	2.1	3.5	7	17	23	39.3
Hulburt ³	4.4	1.7	2.3	3.7	19	30.3	57.2
Sullivan ⁵	5.8	3.3	—	—	27.2	35.1	64.8
Dorsey ⁷	7.6	2.2	2.4	3.6	17	28	56
Irvine and Pollack ²⁴	10	2	2.5	3.5	15	25	60
Tyler <i>et al.</i> ⁹	3.6	3.6	4.6	7.4	22.5	38	62
Hale and Querry ²⁵	5.8	2.8	2.5	4.5	23	32	60
Kopelevich ¹⁰	0.6	0.3	0.6	3.5	20		
Querry <i>et al.</i> ¹²		3.7	4.5	7.6	26	34	
Tam and Patel ¹⁴		2.30	2.33	5.7	20.5	32.4	59
Ravisankar <i>et al.</i> ²³		1.83	3.18	6.9	27.8	—	—

Most of these errors are eliminated in the photo-acoustic method adopted by Tam and Patel¹⁴ for absorption measurements and in the split-pulse laser method by Querry *et al.*¹², for attenuation measurements. The values reported by Tam and Patel seem to be the most reliable set for the absorption coefficients for pure water in the visible region. They are shown in Table 3, for certain wavelengths. The minimum value of absorption according to them is in the region around 470 nm where $a = 0.00017 \text{ cm}^{-1}$. Later Ravisankar *et al.*²³ observed the minimum attenuation (which includes scattering also) in the region 435 to 455 nm while in the same region Tam and Patel had observed a rise in the absorption. The disparities in these results can be because of the very low value of absorption involved.

There are very few reports^{35,36} of absorption measurements in the region 200 to 400 nm. Here also, there are disagreements in the results although the magnitude of absorption is one order higher than that in the visible region. The values given by Hale and Querry²⁵ from the review work seem to be more reliable and they are also reproduced in Table 3. To our knowledge there is no experimental data reported, in the past two decades on the absorption of water in this region. It can be seen from the table that the absorption increases below 400 nm.

The absorption of water below 200 nm is studied by several workers³⁷⁻⁴⁰. The increased absorption in this region is due to the electronic excitation⁴¹ of the H_2O molecule. The absorption coefficient reaches values nearing 500 cm^{-1} . The first electronic transition in H_2O occurs at short wavelengths. It consists of a broad continuum from 186 to 145 nm. It is the tail of this continuum that extends to the blue region of the spectrum. The absorption steadily decreases from 2 cm^{-1} at 186 nm to 0.0006 cm^{-1} at 400 nm.

Table 3. Absorption coefficient $a(\lambda)$ of water for the region 200 to 700 nm as reported by Hale and Querry²⁵ (I) and Tam and Patel¹⁴ (II)

Wavelength (λ) (nm)	Absorption coefficient $a(\lambda) (10^{-4} \text{ cm}^{-1})$ I	Wavelength (λ) (nm)	Absorption coefficient $a(\lambda) (10^{-4} \text{ cm}^{-1})$	
			I	II
200	691	450	2.85	2.30
225	277	475	2.47	1.75
250	168	500	2.50	2.33
275	107	525	3.16	3.90
300	67	550	4.48	5.70
325	41.8	575	7.86	8.05
350	23.3	600	22.8	20.5
375	11.7	625	27.9	29.6
400	5.85	650	31.7	32.4
425	3.84	675	41.5	40.8
		700	60.1	59.0

The overall absorption spectrum of water is shown in Fig.1. On the longer wavelength side (above 500 nm), the absorption is mainly due to the overtone absorption of the $O-H$ vibrations, while the absorption on the shorter wavelength side of (200 to 300 nm) marks the beginning of an electronic absorption continuum. This brings about a relatively broad minimum absorption region from 450 to 480 nm which is usually referred to as the blue-green window. The actual magnitude of absorption in this spectral region and the shape of the absorption curve will be influenced by the chlorophyll content and the bio-organic matter besides the intrinsic absorption due to the water.

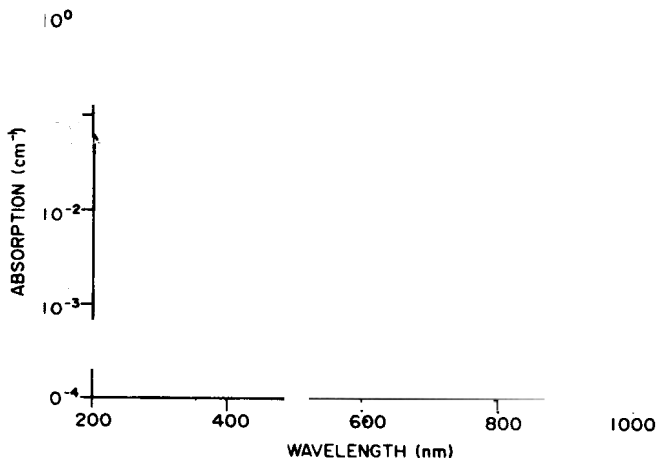


Figure 1. Absorption spectrum of liquid water for the region 200 to 1000 nm.

3. ABSORPTION DUE TO CONSTITUENTS OF OCEAN WATER

The ocean water contains of all possible known elements. However, the concentrations of these elements vary widely with the majority of them present only in traces. A few of the constituents are present in large quantities, which have a considerable influence on the density and these are classified as the major constituents. As far as the absorption of light by sea water is concerned, the major constituents of sea water can be classified into organic and inorganic. The major inorganic compounds remain dissolved in sea water and hence are split into ions. They include Na^+ , Mg^{2+} , Cl^- , SO_4^{2-} , etc. The effect of the major dissolved constituents of sea water on optical attenuation has been very systematically studied by Ravisankar *et al*²³. Their observations in the region 430 to 630 nm by split-pulse laser method conclude that within the concentration levels applicable to sea water, the major and minor dissolved inorganic compounds in sea water do not affect the attenuation in that region. However, there are evidences⁴² to show that the presence of nitrate and bromide ions will enhance the absorption below 220 nm. This topic is not discussed here as the purview of the paper is confined to the blue-green region.

A great deal of study has been conducted on the absorption by the yellow substance in ocean waters. When plant tissue decomposes in the soil or in a water body, most of the organic matter is broken down by microbial action within days or weeks to ultimately carbondioxide and inorganic forms of nitrogen, sulphur and phosphorus. In the course of decomposition, a complex group of polymers is formed which is collectively called humic substances. These humic substances vary in size from freely soluble compounds with molecular weights of a few hundreds to insoluble macromolecular aggregates with molecular weights of hundreds of thousands and perhaps ranging upto millions.

It seems likely that most of the dissolved yellow colour in inland waters is due to soluble humic substances leached from soils in catchment areas. Yellow material

of the humic type can also be generated by decomposition of plant matter within water. This could be of significance in productive water bodies. Kopelevich and Burenkov⁴³ observed strong correlation between the concentration of yellow substance and level of phytoplankton chlorophyll in productive oceanic waters. The absorption spectrum of humic substances is shown in Fig. 2, as reported by Kirk⁴⁴. The absorption is very low in the red end of the visible spectrum and rises steadily with decreasing wavelength. Absorption is still higher in the ultraviolet region.

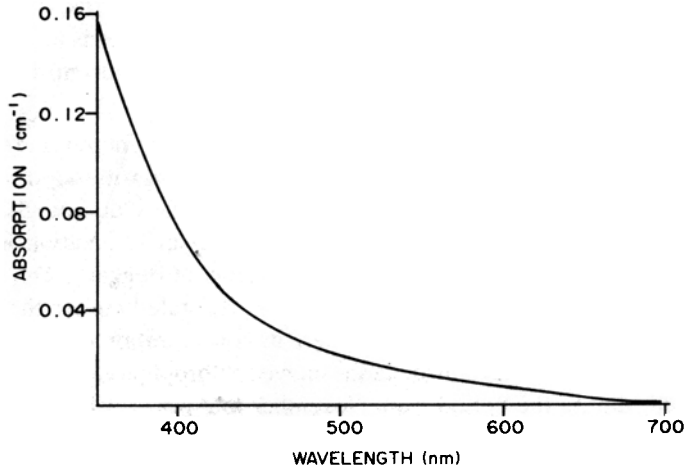


Figure 2. Absorption spectrum of soluble yellow materials (humic substances).

Since most of the humic substances in ocean are due to river discharge⁴⁵, it is reasonable to assume that the concentration of humic substances will be very small at locations far away from the land. In the ocean waters the absorption due to yellow matter⁴⁶ is of the order of 0.0001 to 0.0005 cm⁻¹ at a wavelength of 440 nm.

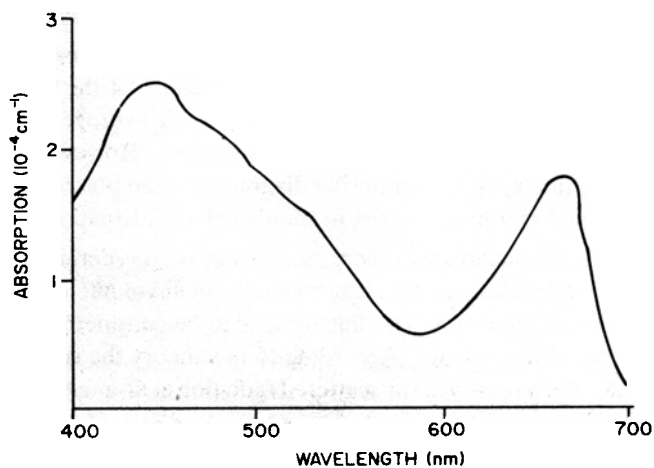


Figure 3. Specific absorption coefficient corresponding to 1 mg chlorophyll-a/m³.

Another source for absorption of light in ocean waters is the chlorophyll. Typical concentration of chlorophyll in ocean waters is in the range 0.05 to 3 mg/m³. Morel and Prieur⁴⁷ were able to arrive at an absorption spectrum (Fig. 3) corresponding to 1 mg chlorophyll-a per cubic metre for oceanic phytoplankton.

In the region 450 to 480 nm, the absorption due to chlorophyll-a for a concentration of 1 mg/m³ is 0.0002 cm⁻¹. It was seen in the earlier section that the absorption of pure water in this region is nearly of the same value. This shows that absorption due to chlorophyll-a is significant at this concentration. In other words, it can be safely concluded that when the total loss of light energy in ocean water is to be calculated, then the absorption by chlorophyll cannot be neglected if the concentration is greater than 0.1 mg/m³.

The concentration of chlorophyll-a varies with location, depth and time of the day and season. Measurements⁴⁸ on chlorophyll distribution with depth in Southern California coastal waters show that the concentration is highest at around 25 m depth. The data collected during the International Indian Ocean Expedition in the early sixties, indicate that a similar situation exists in the Bay of Bengal⁴⁹. The chlorophyll concentration varies randomly in the Arabian Sea. As stated earlier the absorption due to chlorophyll will be significant only where its concentration is above 0.1 mg/m³. In the Indian ocean surface, certain locations showed chlorophyll concentration greater than 0.1 mg/m³, during the period from November to April. Excluding this, the rest of the ocean, at all depths and at all seasons showed less than 0.1 mg/m³ concentration during the years (1964-65) in which the data were collected.

The total absorption coefficient of the aquatic medium at any wavelength is the sum of the absorption coefficients of all the light absorbing components.

4. SCATTERING DUE TO DENSITY FLUCTUATIONS

In addition to absorption, scattering of the light by the medium also takes place as light propagates. Scattering by the pure liquid medium alone is considered in this section, while that by suspended particles will be taken up in the following section.

The scattering theory first described by Lord Rayleigh applies to independently scattering particles. It cannot be applied to liquids because of the strong interaction effects between the molecules particularly in water with hydrogen bonds. It is the fluctuation theory which is more valid in the case of liquids. However, for wavelength dependence, the symmetry of the scattering diagram and the polarization properties, the results so obtained continue to exist in the theory of fluctuations.

In the Einstein-Smoluchowski theory, scattering is considered to be caused by random motion of molecules which in a sufficiently small volume causes fluctuations in density and dielectric constant. The fluctuations to be considered are those whose frequencies are optical frequencies. According to this theory the isotropic part of the Rayleigh ratio (i.e., the intensity of the scattered radiation at an angle 90°) is given by⁵⁰

$$R_{\text{iso}} = \frac{\pi^2}{2\lambda^4} K_B T \beta_T \frac{(n^2 - 1)^2 (n^2 + 2)^2}{9} \quad (3)$$

where K_B is the Boltzmann constant, T is the absolute temperature, β_T is isothermal

compressibility, and n is the refractive index at wavelength λ . This leads to the expression for the scattering coefficient b

$$b = \frac{8 \pi^3}{27 \lambda^4} K_B T \beta_T (n^2 - 1)^2 (n^2 + 2)^2 \quad (4)$$

Experimental study of scattering shows that the electrolyte solution scatters more. This increase is due to the concentration fluctuation term. An approximate calculation by Morel⁵⁰ shows that the sea water of 38 ‰ salinity scatters 34 per cent more than pure water. It can be reasonably assumed that sea water of salinity 35 to 38 ‰ scatters 1.3 times more than pure water. Morel has tabulated the calculated values of scattering coefficients for pure sea water ($S = 35$ to 38 per cent). These are shown in Table 4. shown in Table 4.

It can be noticed that the scattering due to density fluctuations or concentration fluctuations is not a major cause for optical attenuation as the scattering contributes only about 10 per cent of the absorption in the wavelength region greater than 400 nm.

Table 4. Total scattering coefficient for pure and pure sea water of salinity 35.39 ‰ as a function of wavelength λ

Wavelength (λ) (nm)	Total scattering coefficient (b) (10^{-4} cm^{-1})	
	Pure water	Pure sea water
350	1.035	1.345
375	0.768	0.998
400	0.581	0.755
425	0.447	0.581
450	0.349	0.454
475	0.276	0.359
500	0.222	0.288
525	0.179	0.233
550	0.149	0.193
575	0.125	0.162
600	0.109	0.141

5. SCATTERING DUE TO SUSPENDED PARTICLES

The treatment employed by Mie, to derive a rigorous expression for the perturbation of a plane monochromatic wave by spherical non-absorbing particles, is described by Van de Hulst⁵¹. The Mie theory is difficult to comprehend in simple terms. However, the treatment of a monodisperse system of particles of a given refractive index is based on the assumption that the scattered light has the same wavelength as the incident light and the particles are independent. Another simplification often made is that there is no multiple scattering. It can be shown that the scattering coefficient for a monodisperse system b_p is given by

$$b_p = KN \pi r^2 \quad (5)$$

where K is the efficiency factor or the effective area coefficient, N is the number of particles per unit volume and r is the radius of the particles.

For a polydisperse system the scattering is given by

$$b_p = \pi \sum_{i=1}^n K_i N_i r_i^2 \quad (6)$$

$$\text{or } b_p = \pi \int_{r_1}^{\infty} K(r) r^2 dN(r) \quad (7)$$

The scattering coefficient depends on the size of the particular particles and it does not have a direct dependence on wavelength. However the efficiency factor K depends on the relative refractive index and diameter of the particle and the wavelength of radiation.

While the scattering due to density fluctuations or concentration fluctuation shows axial symmetry in angular distribution with a minimum at 90° , the scattered light distribution due to particles scattering shows predominantly forward scattering. In other words, the forward scattering is intensified with increasing particle size. It of course, shows a minimum at 90° indicating that the scattering at this angle is less than backscatter at 180° .

Burt⁵² has shown the variation of the effective area coefficient K as a function of size, wavelength and relative refractive index. With increasing particle sizes, the coefficient increases rapidly for small radii, then it passes a maximum for sizes of same order of wavelength ($K > 3.0$) and tends after some fluctuations, towards a constant value 2 for large sizes irrespective of wavelength. The results of Hodgkinson⁵³ and of Jerlov and Kullenberg⁵⁴ indicate that the value of the effective area coefficient K approaches 2 for particle sizes above $1 \mu\text{m}$. Similar results were obtained by Burt⁵⁵.

A critical review of papers on Mie calculation for polydisperse systems has been given by Kullenberg⁵⁶, who points out that the assumptions of the size distribution are often unrealistic. Brown and Gordon⁵⁷ have tabulated the scattering function for four wavelengths for the cases with refractive index between 1.01 and 1.15 and size ranges 1.017 to $20 \mu\text{m}$. Morel⁵⁸ has provided a comprehensive computation, of the scattering function and its polarization components. According to him, the different parts played by different sizes in total scattering are 10 per cent due to sizes above $100 \mu\text{m}$, 10 per cent due to sizes below $1.1 \mu\text{m}$ and 50 per cent due to those of sizes $5 \mu\text{m}$.

From a comparative study of theoretical and experimental scattering function, Kullenberg⁵⁹ concludes that scattering in Sargasso Sea and Mediterranean Sea is chiefly produced by particles larger than 1 to $2 \mu\text{m}$. This is supported by Brown and Gordon⁶⁰ and by Zaneveld *et al.*⁶¹.

In order to calculate the scattering losses, it is essential to know the size distribution of the particles in the sea water. Direct visual and photographic studies^{62,63} indicated the presence of many large scatterers mostly above 1 mm . There are evidences⁶⁴ to

show that fairly large detrital aggregates are formed in the sea, to which living cells are added. The particle size distributions in coastal waters are not consistent. The Coulter Counter technique, the usually used one, has a tendency to overestimate the number of small particles. In the recent years, laser-based particle size analyzers are available in the market.

An exponential distribution has been suggested for describing a family of marine particles $N = \text{Const. } D^{-\gamma}$, where N is the number of particles larger than size D and the exponent γ is a characteristic constant. The value of γ fluctuates between⁶⁵⁻⁷¹ 0.7 and 6.0 though an average value of N may be estimated⁷² at 2.5.

Investigations conducted by Kitchen *et al.*¹⁹ show that the shapes of the beam attenuation spectra are highly correlated with the slopes of particles size distribution. It would thus be possible to predict the slope of the size distribution with some accuracy from attenuation spectra.

A size distribution⁶⁰ of the form

$$dN/dD = 33,000/D^4 \text{ for } 0.08 < D < 10.0 \mu\text{m} \quad (8)$$

where dN is the number of particles per ml with diameter between D and $D + dD$ in μm was shown to reproduce Kullenberg's⁵⁹ value for the volume scattering function $\beta(\theta)$ for Sargasso Sea at 632.8 nm adequately. The volume scattering function is connected to a scattering coefficient b , by the relation $b = \int_0^{180} \beta(\theta) d\omega$. Using this distribution, and assuming a value of 2 for effective area coefficient, the value of b can be calculated for the Sargasso Sea (which contains the most clear water compared to the rest of the ocean waters). If we consider only the particles above 1 μm size, the value of b_p for Sargasso Sea will be 0.00023 cm^{-1} . The values of b_p for different sea waters observed by different workers are tabulated by Kirk⁷³. These values vary widely with locations from 0.00023 cm^{-1} (at 633 nm) in Sargasso Sea to 0.018 cm^{-1} in San Diego Harbour, California. In Indian Ocean the average value of particle scattering coefficient is shown⁷³ to be 0.0018 cm^{-1} .

The scattering properties of phytoplankton are studied by Morel and Bricaud⁷⁴. They have calculated the efficiency factor for scattering and absorption and the backscattering efficiency of phytoplankton and showed that scattering is depressed by increasing absorption. These studies are of importance in estimating phytoplankton concentration by remote sensing techniques. However this can be a major source of attenuation only in highly productive area.

6. TOTAL BEAM ATTENUATION COEFFICIENT

The total loss of light in the water medium at a particular wavelength will be the sum of all the contributions at that wavelength, assuming no interaction or multiple scattering. The contributions arising out of the above discussed four factors in the wavelength range 400 to 700 nm are plotted in Fig. 4 for comparison. Curve 1 shows the absorption coefficient of water as given by Tam and Patel¹⁴, which is the most reliable set of values available in the literature. Curve 2 represents the absorption due to the chlorophyll present, calculated for the average chlorophyll concentration

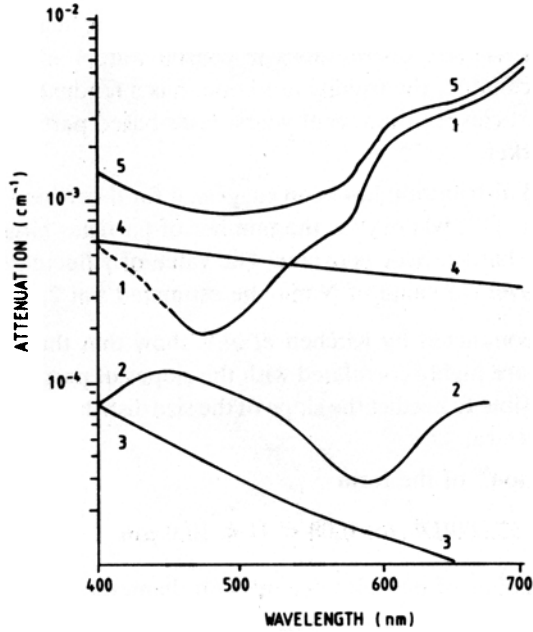


Figure 4. Contribution to total attenuation from different processes. Curve 1—absorption due to liquid water; 2—absorption due to 0.5 mg chlorophyll/m³; 3—scattering due to fluctuations; 4—scattering due to particles; and 5—total attenuation, the sum of individual contributions.

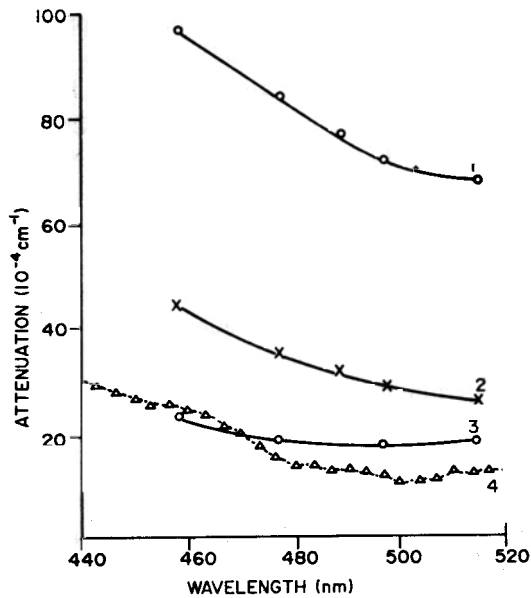


Figure 5. Attenuation of blue-green radiation in ocean waters of different locations. Curve 1—Miramar Beach, Goa; 2—Mandapam coast, Tamilnadu; 3—20 km east of Visakhapatnam and 4—3 km west of Cochin (large particles filtered).

in Indian Ocean, based on the data given by Morel and Prieur⁴⁷. Curve 3 shows the scattering coefficient b_m arising out of fluctuations as discussed in section 4. The scattering loss due to particle scattering is represented by curve 4. These values are based on reports⁷⁵ of measurements in different oceanic stations at 544 nm and assuming a λ^{-1} dependence on wavelength. It has been shown⁵⁸ that in particle dominated natural waters, the value of b varies approximately in accordance with λ^{-1} . Curve 5 shows the total beam attenuation coefficient, that is the sum of individual contributions.

The total beam attenuation coefficients for the blue-green region, of sea water samples collected from different locations are shown in Fig. 5. Only the results of measurements in the blue-green window region are illustrated, to elucidate the behaviour of the window at various locations. Curve 1 shows the variation of attenuation for the sample collected by us from Miramar Beach, Goa. Curve 2 shows the results for water collected by us from Mandapam Coast, Tamilnadu. Curve 3 represents a sample far from the coast, i.e., 20 km to the east of Visakhapatnam, collected by Naval Science and Technological Laboratory. For curve 4, the sample is collected by us from a place 3 km to the west of Cochin. The measurements on Cochin sample were done after filtering of large size particles.

The highest attenuation is shown by the coastal water from Goa. This may be due to the high density of suspended particles. Far from the coast, the concentration of suspended particles will be greatly reduced. This is the main reason for smaller attenuation shown by other samples.

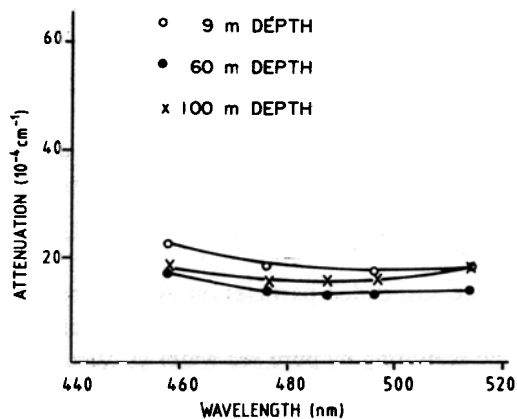


Figure 6. Attenuation of blue-green radiation in ocean waters of different depths. (samples from Bay of Bengal, 20 km to the east of Visakhapatnam).

The variation in the attenuation coefficient with depth will occur in locations where there is drastic depth dependence or chlorophyll concentration. A recent study conducted in sea water samples collected at different depths of Bay of Bengal indicates that there is no significant variation in the attenuation with depth (Fig. 6). The results

of the International Indian Ocean Expedition⁴⁹ show that the chlorophyll concentration in Bay of Bengal, in most of the locations at all seasons is less than 0.1 mg/m^3 . Therefore the effect of chlorophyll will be less significant there. This can be one of the reasons for the constant behaviour of attenuation coefficient with depth.

7. CONCLUSIONS

As can be seen in Fig. 4, the major contribution to attenuation near coastal waters is from scattering due to suspended particles in ocean water. The inherent absorption and scattering by water and those by organic and inorganic compounds present in the ocean water play relatively a less significant role in the region below 550 nm.

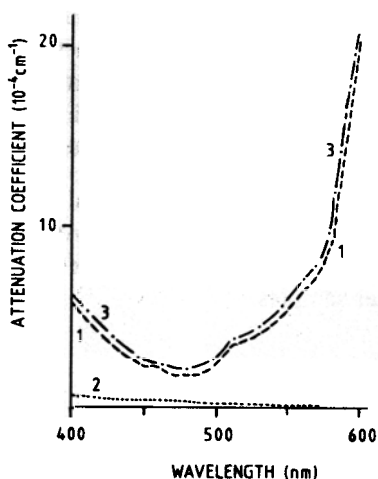


Figure 7. Attenuation by pure sea water. Curve 1—absorption by water; 2—scattering by pure sea water (Morel⁵⁰); and 3—total attenuation, the sum of curves 1 and 2.

The influence of the suspended particles on attenuation is further illustrated in Figs. 7 and 8. Curve 1 of Fig. 7 is the absorption spectrum of pure water reproduced. Curve 2 represents the scattering by pure sea water as calculated by Morel⁵⁰. It is to be remembered that Morel's results for scattering coefficient are for pure sea water in solution form, which is devoid of suspended particles. The total beam attenuation coefficient which is the sum of curves 1 and 2 is also shown in the Fig. 7 as curve 3. The maximum transmission is centred around 475 nm in the pure particle-free sea water. Since it is the absorption due to water that plays a major role here, the scattering being negligible, the presence of the window in this region can be explained using the same arguments which we had for pure water, i.e., the overtone absorption of the $O-H$ vibrations causes high attenuation in the red part of the spectrum, while the electronic excitation of H_2O molecule results in the high absorption in the ultraviolet

region. Thus a minimum appears in between, at around 475 nm which we term as blue-green window.

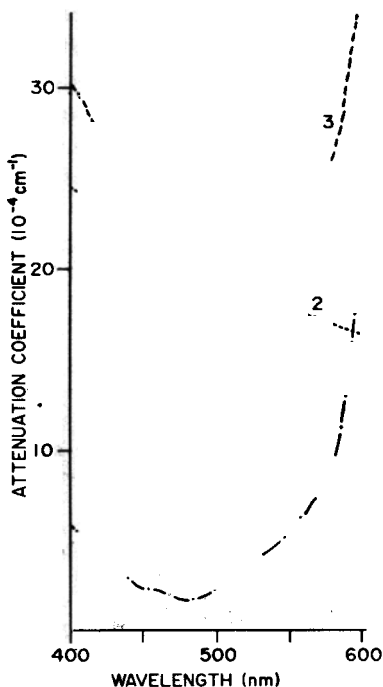


Figure 8. Attenuation by sea water containing suspended particles. Curve 1—absorption by pure water; 2—scattering coefficient deduced from Kopelevich and Burenkov⁷⁴ for Indian Ocean; and 3—total attenuation, the sum of curves 1 and 2.

In Fig. 8, the case of a sea water sample with suspended particles is considered. The absorption due to pure water is given as curve 1. Curve 2 represents the scattering coefficient. This curve is deduced from the reports of Kopelevich and Burenkov⁷⁴. They obtained the value of b as 0.0018 cm^{-1} at 544 nm as an average value of scattering coefficient from the measurements at 164 oceanic stations in Indian Ocean. Curve 2 is plotted using this value and assuming a λ^{-1} dependence. The total beam attenuation coefficient is plotted as curve 3. It is clear that apart from the change in the magnitude of the attenuation, there is a small but noticeable shift in the window. For pure water, the window was in the region 450 to 500 nm while for this particular sample, it is shifted by about 25 nm towards red.

Comparing Figs. 7 and 8, one can see that the magnitude of attenuation is very strongly depending on the particles present in the sea water. The set of values plotted in Fig. 8 for scattering is not an extreme set. Values of b tabulated by Kirk⁷³ from various reports indicate that it can be one-eighth of these values in clear sea like Sargasso Sea, or can be four times higher as observed in English Channel, or even ten times higher as found in San Diego harbour.

The effect of Chlorophyll on the attenuation at different wavelengths is illustrated in Fig. 9. Curve 1 is absorption due to pure water. Curve 2 represents absorption due to chlorophyll for a concentration of 5 mg/m^3 . This is a high value compared to the average value of chlorophyll content observed in ocean water. In spite of this, we have chosen this concentration, in order to understand the general trend in the behaviour of the window due to the presence of chlorophyll. It can be seen that in the total beam attenuation curve, the minimum is centred around 550 nm. Thus the presence of chlorophyll also pushes the minimum wavelength region to longer wavelength side. It is evident that the magnitude of this shift will depend on the concentration of chlorophyll.

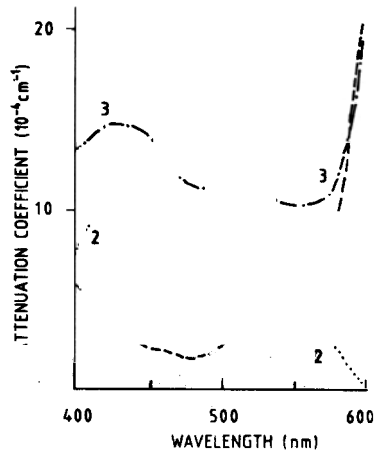


Figure 9. Attenuation by sea water containing chlorophyll. Curve 1—absorption by pure water, 2—absorption by chlorophyll 5 mg/m^3 ; and 3—total attenuation, the sum of curves 1 and 2.

Based on the report of the International Indian Ocean Expedition⁴⁹ where it is pointed out that the chlorophyll concentration in Indian Ocean was everywhere less than 0.5 mg/m^3 , which is one-tenth of the value which we used to plot the curve 2 of Fig. 9, it is safe to conclude that the chlorophyll is not going to play a dominant role in the attenuation spectrum for a vast area in this region of the sea. However, in certain locations where the productivity is more, the presence of chlorophyll will have to be considered.

Thus we can state that the clearer the water, the greater is the transmission in the blue region of the spectrum. The presence of dust particles and/or chlorophyll, will shift the window towards longer wavelength in addition to increasing the magnitude of attenuation.

It therefore turns out that if more reliable values of optical attenuation in our ocean waters are to be predicted, more accurate measurements of the particle density, size distribution and chlorophyll content, as a function of the location, depth and season are necessary.

Origin of Blue-Green Window

However, if one is interested in obtaining the attenuation coefficients, it is always desirable to measure it *in situ* or on board a ship. There are several reports of laboratory measurements of attenuation of collected sea water samples. The organic matter, such as chlorophyll, etc. in the stored sea water samples, will degrade within few weeks. Thus it will not represent the true characteristics of actual ocean or sea water. Because of these reasons, only the values obtained by *in situ* studies or those measured within a few hours after collection can be considered reliable. There will be diurnal and seasonal variations in the constituents of sea water which also have to be taken into account. The split-pulse laser method is one of the best experimental techniques which can be employed on board to measure the absolute values of attenuation coefficient. The photoacoustic technique is ideal for absorption by pure water but as the contribution from scattering becomes significant, it is not known as to what its accuracy will be.

ACKNOWLEDGEMENTS

The authors thank Commodore S. Rao and Lt. Cmdr. S.K. Bannerjee, Naval Science and Technological Laboratory, Visakhapatnam for the fruitful discussions and technical service rendered by them and for providing sea water samples from different depths of Bay of Bengal. Thanks are also due to Prof. K.I. Vasu and Dr. Anand of CECRI, Karaikudi for their help in collecting certain samples. The authors acknowledge the help rendered by Dr. B.N. Desai, Director, National Institute of Oceanography (NIO), Goa, for making available some relevant literature and to Dr. L.V.G. Rao and Dr. A.H. Parulekar, NIO, for the discussions the authors had with them. We have to thank also Dr. V.K. Aatre, Director, NPOL for some useful discussions.

The financial support by Defence Research and Development Organisation is gratefully acknowledged.

REFERENCES

- James, H.R. & Birge, E.A., *Trans. Wis. Acad. Sci. Arts Lett.*, **31**(1938), 1-154.
- Clarke, G.L. & James, H.R., *J. Opt. Soc. Am.*, **29**(1939), 43-55.
- Hulburt, E.O., *J. Opt. Soc. Am.*, **35**(1945), 698-705.
- Curcio, J.A. & Petty, C.C., *J. Opt. Soc. Am.*, **41**(1951), 302-304.
- Sullivan, S.A., *J. Opt. Soc. Am.*, **53**(1963), 962-967.
- Drummer Jr., L.F. & Knestrick, G.L., *Appl. Opt.*, **6**(1967), 2101-2103.
- Dorsey, N.E., *Properties of Ordinary Water-Substance*, (Hafner, New York), 1968.
- Zolotarev, V.M., Mikhailov, B.A., Aperovich, L.I. & Popov, S.I., *Opt. Spectrosc.*, **27**(1969), 430-432.
- Tyler, J.E., Smith, R.C. & Williams, W.H., *J. Opt. Soc. Am.*, **62**(1972), 83-91.
- Kopelevich, O.V., *Opt. Spectrosc.*, **41**(1976), 391-392.

11. Hass, M. & Davisson, J.W., *J. Opt. Soc. Am.*, **67**(1977), 622-624.
12. Querry, M.R., Cary, P.G. & Waring, R.C., *Appl. Opt.*, **17**(1978), 3587-3592.
13. Bukata, R.P., Jerome, J.H., Bruton, J.E. & Jain, S.C., *Appl. Opt.*, **18**(1979), 3926-3932.
14. Tam, A.C. & Patel, C.K.N., *Appl. Opt.*, **18**(1979), 3348-3358.
15. Wilson, W.H., *Proc. SPIE.*, **208**(1979), 64-72.
16. Tsubomura, H., Yamamoto, N., Matsuo, N. & Okada, Y., *Proc. Japan Acad. Ser. B*, **56**(1980), 403-407.
17. Smith, R.C. & Baker, K.S., *Appl. Opt.*, **20**(1981), 177-184.
18. Mercier, H., Gaillard, F., Cariou, J. & Lotrian, J., *J. Phys. D.*, **15**(1982), 563-569.
19. Kitchen, J.C., Zaneveld, J.R.V. & Pak, H., *Appl. Opt.*, **21**(1982), 3913-3918.
20. Romanov, N.P. & Shuklin, V.S., *J. Sov. Laser Res.*, **5**(1984), 75-77.
21. Wie Saizhen, Cai Shoufu, Ying Xiaohong & Cheng Gensong, *J. Zhefiang. Univ. (China)*, **18**(1984), 72-80.
22. Ravisankar, M., Reghunath, A.T., Sathianandan, K. & Nampoori, V.P.N., *In Proceedings of the IV Quantum Electronics Symposium, Cochin, (DAE, India), 1986*, pp. 142-143.
23. Ravisankar, M., Reghunath, A.T., Sathianandan, K. & Nampoori, V.P.N., *Appl. Opt.*, **27**(1988), 3887-3894.
24. Irvine, W.M. & Pollack, J.B., *Icarus*, **8**(1968), 324-360.
25. Hale, G.M. & Querry, M.R., *Appl. Opt.*, **12** (1973), 555-563.
26. Jerlov, N. & Steeman-Nielson, E. (Eds), *Optical Aspects of Oceanography*, (Academic Press, New York), 1974.
27. Jerlov, N.G., *Marine Optics*, (Elsevier, Amsterdam), 1976.
28. Tyler, J.E. (Ed.), *Light in the Sea*, (Dowden, Hutchinson & Ross, Stroudsburg), 1977.
29. Yura, H.T., *Appl. Opt.*, **12**(1973), 108-115.
30. Preisendorfer, R.W., *In Light in the Sea*, Tyler, J.E. (Ed), (Dowden, Hutchinson & Ross, Stroudsburg), 1977, pp. 46-64.
31. Austin, R.W. & Petzold, T.J., *Opt. Eng.*, **25**(1986), 471-479.
32. Bayly, J.G., Kartha, V.B. & Stevens, W.H., *Infrared Phys.*, **3**(1963), 211-222.
33. Robertson, C.W. & Williams, D., *J. Opt. Soc. Am.*, **61**(1971), 1316-1320.
34. Rusk, A.N., Williams, D. & Querry, M.R., *J. Opt. Soc. Am.*, **61**(1971), 895-903.
35. Dawson, L.H. & Hulburt, E.O., *J. Opt. Soc. Am.*, **24**(1934), 175-177.
36. Lenoble, J. & Saint Gully, B., *Compt. Rend.*, **240**(1955), 954-955.
37. Watanabe, K. & Zelikoft, M., *J. Opt. Soc. Am.*, **43**(1953), 753-755.
38. Halmann, M. & Platzner, I., *J. Phys. Chem.*, **70**(1966), 580-581.
39. Berrett, J. & Mansell, A.L., *Nature*, **187**(1960), 138.

40. Price, W.C., Harris, P.V., Beaven, G.H. & Johnson, E.A., *Nature*, **188**(1960), 45-46.
41. Herzberg, G., *Molecular Spectra and Molecular Structure, Vol. III : Electronic Spectra and Electronic Structure of Polyatomic Molecules*, (Von Nostrand, Princeton), 1966, pp. 488-489.
Ogura, N. & Hanya, T., *Nature*, **212**(1966), 758.
43. Kopelevich, O.V. & Burenkov, V.I., *Oceanology*, **17**(1977), 278-282.
44. Kirk, J.T.O., *Aust. J. Mar. Freshwater Res.*, **27**(1976), 61-71.
45. Hojerslev, N., *In 17th General Assembly of IAPSO (Canberra), 1979, Abstracts*, p.71.
46. Kirk, J.T.O., *Light and Photosynthesis in Aquatic Ecosystems*, (Cambridge University Press), 1983, pp. 57-59.
Morel, A. & Prieur, L., *Limnol. Oceanogr.*, **22**(1977), 709-722.
48. Lieberman, S.H., Gilbert, G.D., Seligman, P.F. & Diebelka, A.W., *Deep-Sea Res.*, **31**(1984), 171-180.
49. *Atlas of the International Indian Ocean Expedition—Phytoplankton Production*, (Institut fur Meereskunde-Kiel Univ.), 1976.
50. Morel, A., *In Optical Aspects of Oceanography*, Jerlov, N. and Steeman-Nielson, E. (Eds.), (Academic Press, New York), 1974, pp. 1-24.
51. Van de Hulst, H.C., *Light Scattering by Small Particles*, (Wiley, New York), 1957; pp. 114-130.
52. Burt, W.V., *J. Mar. Res.*, **15**(1956), 76-80.
53. Hodkinson, J.R., *In ICES Electromagnetic Scattering*, Kerker, M. (Ed.), (Pergamon, London), 1963, pp. 87-100.
54. Jerlov, N.G. & Kullenberg, B., *Tellus*, **5**(1953), 306-307.
55. Burt, W.V., *Tellus*, **6**(1954), 229-231.
56. Kullenberg, G., *In Optical Aspects of Oceanography*, Jerlov, N.G. & Steeman-Nielson, E. (Eds.), (Academic Press, New York), 1974, pp. 25-49.
57. Brown, O.B. & Gordon, H.R., *Tables of Mie Scattering Function for Low Index Particles Suspended in Water*, (Univ. of Miami, Opt. Phys. Lab.), 1972, MIAPH-OP-71.5.
58. Morel, A., *In Light in the Sea*, Tyler, J.E. (Ed.), (Dowden; Hutchinson & Ross, Stroudsburg), 1977, pp. 65-97.
59. Kullenberg, G., *Deep-Sea Res.*, **15**(1968), 423-432.
60. Brown, O.B. & Gordon, H.R., *Appl. Opt.*, **12**(1973), 2461-2471.
61. Zaneveld, J.R.V., Roach, D.M. & Pak, H., *J. Geophys. Res.*, **79**(1974), 4091-4095.
62. Nizhizawa, S., Fakuda, M. & Inoue, N., *Bull. Fac. Fish.*, (Hokkaido University), **5**(1954), 36-40.
63. Costin, J.M., *J. Geophys. Res.*, **75**(1970), 4144-4150.

64. Krey, J., *J. Cons., Cons. Perm. Int. Explor. Mer.*, **26**(1961), 263-280.
65. Kullenberg, B., *Tellus*, **5**(1953), 302-305.
66. Jerlov, N.G., *Tellus*, **5**(1953), 59-65.
67. Ochakovsky, Yu.E., *U.S. Dept. Comm., Joint Publ. Res. Ser. Rep.*, **36**(816), (1966), 98-105.
68. Gordon Jr., D.C., *Deep-Sea Res.*, **17**(1970), 175-185.
69. Sheldon, R.W., Sutcliffe Jr., W.H. & Prakash, A., *Limnol. Oceanogr.*, **18**(1973), 719-733.
70. Brun-Cottan, J., *Cah. Oceanogr.*, **23**(1971), 193-205.
71. Matsumoto, E. & Nakamotu, N., *In Preliminary Report of the Hakuho Maru Cruise KH-71-3 (IBP Cruise), June 18 to July 29, 1971, (Ocean Research Institute, University of Tokyo), 1973, pp. 61-62.*
72. Jerlov, N.G., *Marine Optics*, (Elsevier, Amsterdam), 1976, p. 26.
73. Kirk, J.T.O., *Light and Photosynthesis in Aquatic Ecosystems*, (Cambridge University Press), 1983, pp. 85-86.
74. Kopelevich, O.V. & Burenkov, V.I., *Izv. Atmos. Oceanic. Phys.*, **7**(1971), 835-840.
75. Morel, A. & Bricaud, A., *In Oceanography from Space*, Gower, J.F.R. (Ed.), (Plenum, London), 1981, pp. 313-327.